Surface & Coatings Technology 388 (2020) 125560

Contents lists available at ScienceDirect

Surface & Coatings Technology

journal homepage: www.elsevier.com/locate/surfcoat

Time-stable wetting effect of plasma-treated biodegradable scaffolds functionalized with graphene oxide

A. Lipovka[a], R. Rodriguez[a,*], E. Bolbasov[b,d,e], P. Maryin[b], S. Tverdokhlebov[b,*], E. Sheremet[c]

[a] Research School of Chemistry & Applied Biomedical Sciences, Tomsk Polytechnic University, Tomsk, Russia
[b] School of Nuclear Science & Engineering, Tomsk Polytechnic University, Tomsk, Russia
[c] Research School of High-Energy Physics, Tomsk Polytechnic University, Tomsk, Russia
[d] V.E. Zuev Institute of Atmospheric Optics SB RAS, Tomsk, Russia
[e] National Research Tomsk State University, Tomsk, Russia

ARTICLE INFO

Keywords:
Biodegradable scaffolds
Graphene oxide
Plasma-treated
Functionalizatyion
Wetting

ABSTRACT

The polymer scaffolds surfaces are inherently hydrophobic what limits its performance as implants and compatibility with human tissue essential for such applications as tissue engineering, nerve regeneration, drug delivery, *etc.* The plasma treatment was demonstrated to change the wetting properties of scaffolds making them hydrophilic. However, that is not a lasting effect. In this work, we aim at addressing this problem with systematic time-stability investigation of scaffolds functionalized with graphene oxide (GO) layers. To this end, we used several polymers including polycaprolactone (PCL), poly-L-lactic acid (PLLA), L-lactide-*co*-glycolide copolymer (PLGA) and L-lactide-co-caprolactone copolymer (PLC) functionalized with GO, evaluating also control samples without any treatment and treated by plasma. Our results demonstrate that the GO coating provides a successful and stable hydrophilic functionality to all polymer scaffolds here investigated. Contrary to plasma treatment used as a reference for the surface-wettability provider, only the GO effects remain stable for extended periods of up to 30 days. This work contributes to the robust application of graphene-functionalized polymer scaffolds with long lifetime hydrophilicity.

1. Introduction

Tissue engineering is an alternative to transplantation for the recovery of the damaged organs and tissues gave rise to the development of artificial structures called scaffolds. Scaffolds are 3D porous fiber matrices that serve as the mechanical framework for cells. To form a full-fledged tissue with time stability, scaffolds have to satisfy serious requirements: biocompatibility and lack of immunological rejection, the adhesive surface to promote cell proliferation, porosity, and non-toxicity. These materials include bioresorbable aligned aliphatic polyether nanofibers such as polycaprolactone (PCL), polylactic acid (PLA), polyglycolic acid (PGA), and their copolymers formed by electrospinning [1–3]. The reasons these synthetic polymers are commonly used in tissue engineering are: firstly - their multiple properties and advantages such as good mechanical strength, low immunogenicity, and biocompatibility that allow them to be implanted to human's body. Secondly, these polymers have tunable full degradation to H_2O, CO_2, and other by-products after performing their function in the body during a reasonable time (relative to natural polymers) ranging from several weeks to years [4].

Electrospinning allows bringing out polymer nanofibers with diameters varying from nano to micrometers using a simple single processing step. The other manufacturing advantages, which made electrospinning attractive are the scalability and opportunity to adapt the parameters/process and composition including adding bioactive materials to tailor the polymer for a particular application [5].

However, the main inevitable limitation of all synthetic electrospun scaffolds used in biomedicine is their poor hydrophilicity and low surface energy [6]. Low wettability, surface energy are critical factors that affect the ability to initiate cell adhesion, proliferation, and differentiation required for biomedical and drug delivery applications, also contributing to lengthening the degradation period [7,8]. There is several treatment approaches proposed to influence surface hydrophilicity while introducing additional functional groups to the surface. These surface treatments include modification of synthetic polymers with natural materials like chitosan [9] or silk fibroin [10], chemical treatment using organic solvents [11], aminolysis [12] and hydrolysis [13]. However, the most widespread, diversified and developed method

* Corresponding authors.
E-mail addresses: raul@tpu.ru (R. Rodriguez), tverd@tpu.ru (S. Tverdokhlebov).

https://doi.org/10.1016/j.surfcoat.2020.125560
Received 21 October 2019; Received in revised form 15 January 2020; Accepted 2 March 2020
Available online 05 March 2020

is plasma treatment [14,15].

Given the structural features and physicochemical properties of the scaffolds, reactive magnetron sputtering was demonstrated to be an efficient way to improve the wettability of polymer scaffolds by producing thin coatings on the surface of complex implants without violating the structural integrity of the medical device [16]. This method allows to vary the properties of the resulting coating by changing such parameters as the working gas composition, target material, power at the power source [17]. The wettability changes occur due to the change of the surface chemical structure and the formation of a thin coating of complex composites like titanium oxides, titanium oxynitrides, and titanium nitrides [18]. After plasma treatment, scaffolds show impressive surface modifications. These improvements include enhanced wettability, high surface energy values, and better adhesion while maintaining the same crystallinity and mechanical properties of the bulk material. These effects are a consequence of the polymer surface cleaning from the impurities and changing of chemical composition by the incorporation of polar functional groups on the treated side, typically carboxyl or amine depending on the working gas [19].

Despite the significant changes in the surface characteristics of polymer scaffolds by plasma treatment, it is well-known that the hygroscopic effect is not stable over time. Plasma-treated polymers return to hydrophobic day by day, what is also called the aging process. This process depends on various parameters starting from the polymer type and crystallinity to the environmental conditions [14,20].

On the other hand, carbon nanomaterials such as graphene, carbon nanotubes, and their derivatives are getting more attention for the enhancement of mechanical, thermal, electrical, and other properties including wettability of different surfaces in such applications as bone, dental and tissue engineering, nerve regeneration, and drug delivery systems [21,22]. Graphene oxide (GO) is a promising candidate to prolong the plasma effect as its flakes are highly hydrophilic and stable due to the presence of carboxylic acid groups that provide negative surface charge and, therefore, stability in polar solutions [23]. GO represents the oxidized form of graphene with a layered structure, but containing randomly-distributed epoxy, hydroxyl, carbonyl, phenol, and carboxyl functional groups [24]. These oxygen-containing groups drastically enhance cell-adhesion of different surfaces functionalized with GO as shown in previous work [25]. In terms of scaffolds surface treatment, GO has already served as a platform to bind proteins to stem cells [26]. It was also reported that GO promoted adhesion and differentiation of certain stem cells [27]. Moreover, in a recent work, GO on PLGA surface was used for applications in gene delivery, forming a substrate for stem cells growth and differentiation [28].

Despite these recent applications, it is not yet clear if GO can fasten the plasma hydrophilic effect providing time stability, and if so, we do not know yet for how long this hydrophilicity lasts. Knowing this would be highly helpful especially for long-term applications involving binding drugs or cells to implants. Therefore, through this work, we aim to investigate if the problem of limited time-stability of wettability in biodegradable polymers can be solved by simple surface functionalization with graphene oxide, without adding polymer manufacturing complications. This is the first systematic investigation of the time dependence stability of GO-functionalized polymer scaffolds that could make an impact in future optimization and developments of graphene/polymer heterostructures for biomedical applications.

2. Experimental

2.1. GO preparation

The coating material is GO water dispersion ("Graphenea") prepared by the conventional modified Hummers method [31] with the flake lateral size of less than 10 μm, 2.2–2.5 pH, and 0.4 wt% concentration. Before the deposition on polymers' surfaces, GO was sonicated for 30 min to break up possible aggregates and restore the dispersion homogeneity.

2.2. Scaffolds preparation

Preparation of scaffolds was performed by electrospinning using a NANON-01A unit (MECC Co., Japan). A 200 mm length metal cylinder with a diameter of 100 mm rotating at 200 rpm was used as the collector. For the fabrication, the following parameters were used: 4 ml/h spinning solution consumption, 25 kV voltage, 18G needle, the distance kept between needle and collector was 19 cm.

To prepare the PCL (Sigma Aldrich, UK $M_n \sim 80.000$) spinning solutions, hexofluoroisopropanol ($C_3H_2F_6O$) (Sigma Aldrich, UK) was used. The polymer concentration in the spinning solution was equal to 5 mass %.

The other polymers used for the present work were (with the polymer concentration, mass %): L-lactide-co-caprolactone copolymer (PLC) Purasorb® PLC 7015 (Corbion, Netherlands) - 8%, poly-L-lactide (PLLA) Purasorb® PL 38 (Corbion, Netherlands) - 4%, and L-lactide-co-glycolide copolymer (PLGA) Purasorb® PLG (Corbion, Netherlands) - 2.5%.

2.3. Plasma treatment

For plasma treatment, we used the magnetron sputtering system described earlier [16]. Plasma treatment of biodegradable scaffolds was carried out by DC reactive magnetron sputtering of a titanium (99.999%) target in a nitrogen atmosphere (99.999%). The treatment was performed for 60 s at a discharge power of 40 W.

2.4. GO deposition

The GO functionalization was performed at room conditions by drop coating 100 μl of the GO dispersion over 3 cm^2 of the scaffolds' surface. Before the study, the samples were dried for 12 h under normal conditions.

2.5. Contact angle (CA) measurements

The wettability experiments were done using a Krüss Drop Shape analyzer unit in a laboratory conditions. For the CA measurements we investigated four polymer types divided to the following groups for each: control sample (1 piece), plasma treated sample (5), plasma treated GO functionalized (5), GO functionalized (5). Each sample has a lateral size about 5 × 1.5 cm. For each sample, 3 different points were examined using 3 μl drop of one polar liquid – water. The drop was allowed to sit for 1 min before recording the contact angle. The same procedures were repeated for the monitoring purposes after 1, 4, 8, 15, and 30 days after GO deposition.

2.6. Scanning electron microscopy

The samples morphology was examined through the SEM image analysis using a Quanta 200 3D, FEI, Hillsboro, ORUSA system. Scaffolds were first covered with a thin gold layer by the magnetron sputtering system (SC7640, Quorum Technologies Ltd., UK) to minimize surface charging. The images were obtained under high vacuum, U = 10 kV, and x500, x5000, and x15000 magnification.

2.7. Raman spectroscopy

Raman spectra were obtained using the DXR2Xi Raman Imaging Microscope from Thermo Fisher Scientific U.S. with x100 objective. The samples were irradiated using an infrared laser with the wavelength $\lambda = 785$ nm using powers of 0.5 mW as higher power could lead to the surface modification of polymers and especially the GO films reduction.

2.8. Fourier-transform infrared spectroscopy (FTIR)

Infrared transmission spectra were recorded using Nicolet 5700 (Thermo Electron Corporation, USA) spectrometer within 4000–400 cm^{-1} spectral range. Both GO covered plasma-treated and non-covered plasma-treated samples were investigated.

3. Results and discussion

3.1. PCL

For the investigation of scaffolds wetting behavior, we chose one of the most commonly used synthetic polymers - polycaprolactone (PCL) as it is elastic, proved to be non-toxic, and successfully integrated into biomedical applications. Compared to other polymers, PCL has a longer degradation rate and therefore, is often used as an implant or for long-term drug delivery systems [29].

We performed month-long monitoring of PCL scaffolds wettability behavior separating the polymer samples into several control groups using all possible combinations of preparation methods:

- Pure electrospun PCL scaffolds with no surface modifications;
- Plasma-treated PCL scaffolds;
- Pure PCL scaffolds covered with GO (no plasma treatment);
- Plasma-treated PCL scaffolds covered with GO.

During the whole contact angle monitoring period, we observed the following tendency. Pure PCL was taken as the reference, which remained highly hydrophobic during the 30 days period since no surface modifications were applied. The plasma-treated samples showed remarkable surface changes illustrated by contact angle values close to zero. However, the contact angle started to increase rapidly after seven days from the deposition keeping the same tendency until the end of the monitoring period. By the end of the month, the contact angle rose to 87 ± 9°, a significant change compared to the 0° contact angle value observed right after plasma treatment.

Both GO-covered sample groups exhibited initial contact angle values of about 30°. Considering that the polar groups contribute the most to the surface hydrophilicity, then the contact angles suggest that GO provides fewer polar groups than plasma treatment. Noticeably, both GO-coated sample groups kept the initial values roughly constant during the whole month (Fig. 1). This result illustrates the good stability of GO hydrophilic properties in time, that added to GO mechanical stability [23], make GO-functionalization beneficial for future practical applications of polymer scaffolds.

The contact angle values difference between plasma-treated, GO-coated, and non-coated PCL at the end of the month is 49° ± 2°. The more efficient way to prolong and stabilize the surface hydrophilicity involves functionalization of the preliminary plasma-treated surface; otherwise, the untreated polymer hydrophobicity limits the homogeneous GO distribution compromising the final wettability.

Considering the results of CA measurements for all polymer scaffold types that is clear that GO is responsible for the wettability changes, thus it might seem that preliminary plasma treatment is not necessary to get the effect. However, the covering of the untreated scaffolds with GO water dispersion was trapped because of the high initial hydrophobicity of the materials. That instigated inhomogeneous dispersion distribution, and therefore the formation of heterogeneous covering containing “islands” after drying. At the “islands” where the GO incorporation was performed successfully, the CA values were close to the ones of the treated polymers (Fig. 1). Contrary to untreated surfaces, scaffolds treated with a magnetron discharge plasma could be easily soaked with the aqueous dispersions, therefore the homogeneous GO layer is formed.

Morphology of all samples was investigated by SEM (Fig. 2). The images demonstrate that highly porous PCL scaffolds contain randomly oriented fibers with a diameter varying from 0.5 to 3 μm (Fig. 2a). After plasma treatment, the fiber diameter slightly changes locally due to plasma etching (Fig. 2b), and no more structural changes take place. Multiple layers of GO on the top of the scaffolds form a hydrophilic coating on the fibers looking like a veil (Fig. 2c). Scaffolds have oxygen-containing groups on the surface and charge positively in acidic environment, therefore in the case of GO deposition electrostatic sorption of components on the fibers takes place. It could be noticed that the dispersion does not penetrate inside providing only surface properties changes protecting the unmodified bulk material.

For the investigation of surface changes, we exploit FTIR and Raman spectroscopy (Fig. 3). FTIR allows identifying the chemical composition changes after functionalizing the scaffolds with GO. The FTIR spectra in Fig. 3a is dominated by the signal from the whole scaffold making the minimal contribution from the plasma-treated surface insignificant with respect to the pristine sample. Therefore, we focus on the spectral differences between plasma-treated and GO-treated samples. In both cases, the PCL distinctive stretching modes can be identified in the FTIR spectra in Fig. 3a. PCL polymers demonstrate noticeable peaks at 2933 cm^{-1} and 2861 cm^{-1} responsible for asymmetric and symmetric CH_2 stretching, respectively. The strong peak at 1720 cm^{-1} originates from carbonyl stretching C═O. Bands at 1240 cm^{-1} and 1186 cm^{-1} are related to asymmetric and symmetric OC-O vibrations, respectively. The peak at 1293 cm^{-1} corresponds to C—O and C—C stretching in the crystalline phase, while the peak at 1157 cm^{-1} originates from C—O and C—C stretching in the amorphous phase [30,31].

GO introduces a broad peak from 3000 cm^{-1} to 3670 cm^{-1} corresponding to typical O—H vibration. The hydroxyl groups may appear from absorbed water molecules or OH from phenol or carboxylic groups. Another smaller peak appearing at 1619 cm^{-1} corresponds to O—H vibrations of water [32]. The other GO-related typical peaks attributed to C═O stretching vibrations (1720 cm^{-1}), C—O from alkoxy group (~1050 cm^{-1}) [33,34] are also present in the scaffold itself.

The proportion between crystalline and amorphous phases in PCL scaffolds before and after GO film deposition shows a change from 0.46 to 0.75 indicating the increase in crystallinity for the functionalized material. GO introduces only additional O—H functional groups to scaffolds. At the same time, there is a significant influence on the long-term wetting properties of the material. This implies that the high scaffolds hydrophilicity is due to these hydroxyl functional groups that allow to efficiently attract water molecules. Simultaneously to the enhanced hydrophilicity, the functionalized material profits from the mechanical properties of GO making the ensemble system much more robust.

Raman spectroscopy (RS) complements FTIR spectroscopy in terms of functional groups vibrations identification as shown in Fig. 3b. The observed PCL peaks correspond to the following vibrations: 911 cm^{-1} - C-COO stretching, 1000–1110 cm^{-1} skeletal stretching, 1270–1320 cm^{-1} CH_2 rocking vibrations, 1405–1470 cm^{-1} symmetric bending CH_2. The peak at 2800 cm^{-1} indicates the crystalline phase, while the one at 866 cm^{-1} is attributed to the amorphous phase. The strong peak at 1720 cm^{-1} corresponds to carbonyl stretching [35].

RS has also been widely exploited for the characterization of graphitic materials. Introducing GO demonstrated the overlap of PCL-related bands and the appearance of two characteristic peaks, D (1332 cm^{-1}) and G (1595 cm^{-1}) bands. D band is related to the disorder in graphitic sp^2 material (distortions, vacancies, *etc.*) and indicates the conversion of sp^2 hybridized carbon atoms to sp^3, while the G band corresponds to E_{2g} symmetry mode from sp^2-hybridized carbon [36]. The I_D/I_G ratio for PCL is equal to 1.26; the higher D peak intensity indicates the structural disorder due to the intensive oxidation during the GO synthesis using the modified Hummer's method [27].

To demonstrate the generality of our findings, we investigated other widely-used polymer scaffold materials. Poly-L-lactic acid (PLLA), L-lactide-*co*-glycolide copolymer (PLGA) and L-lactide-co-caprolactone copolymer (PLC) were divided into the same four control groups.

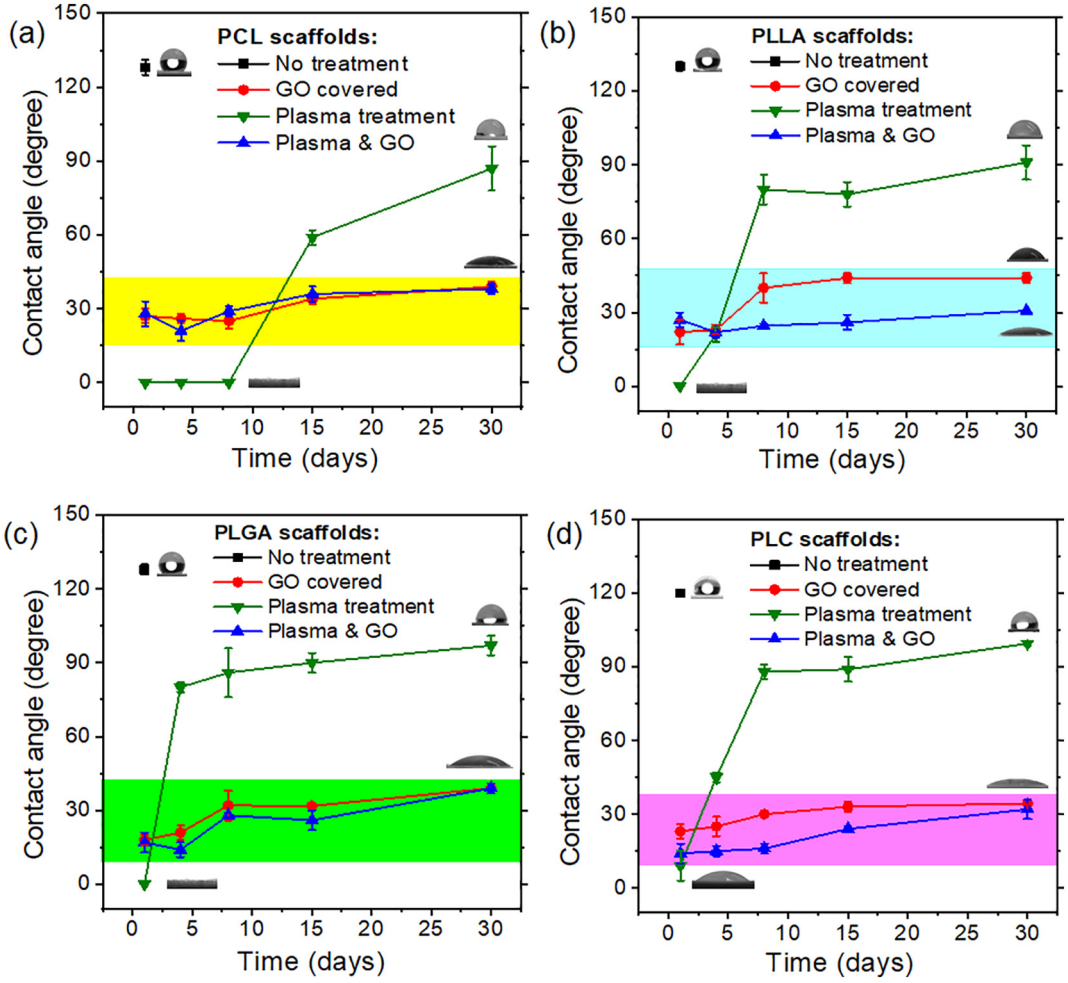

Fig. 1. The dependence of scaffolds wettability from time (in days) for the (a) - PCL, (b) - PLLA, (c) - PLGA, (d) - PLC scaffolds. The testing liquid was distilled water.

3.2. PLLA

PLLA attracted attention in tissue engineering for regenerating cartilage more than other synthetic polymers because the scaffolds degrade to natural metabolites, have mechanical properties similar to cartilage, and good interaction with body cells. Despite that PLLA degradation period corresponds well with healing time, its hydrophobic nature imposes limitations that compromise cell differentiation [37].

The contact angle values using water as a test liquid (Fig. 1b), registered following the same procedure as for PCL, are in agreement with contact angle results obtained on the PCL described above. For the non-functionalized PLLA, the difference is that plasma-treated samples started to recover their intrinsic hydrophobic behavior much sooner than for the case of PCL. This recovery started already from the third day after plasma treatment. At the end of the monitoring period, the difference between GO-coated plasma-treated scaffolds and scaffolds with only plasma treatment was 60° ± 7°.

FTIR spectrum of PLLA (Fig. 4a) demonstrates that the main peaks represent the same functional groups as for PCL, even though some of the peak positions are shifted. Here the significant band at 1743 cm^{-1} corresponds to C═O group stretching vibration, 1182 cm^{-1} and 1081 cm^{-1} are responsible for C-O-C asymmetric and symmetric vibrations respectively. Peaks at 2992 cm^{-1} and 2942 cm^{-1} originate from CH_3 stretching vibrations. Symmetric bending methyl vibrations appear in another spectral range giving rise to the peaks at 1446 cm^{-1} and 1378 cm^{-1}. The described peaks evidence the presence of ester end-capped PLLA scaffold [38].

RS (Fig. 4b) provides the following characteristic bands: 1764 cm^{-1} - carbonyl group stretching vibrations, 1450 cm^{-1} CH_3 asymmetric bending, 1379 cm^{-1}, 1355 cm^{-1}, 1300 cm^{-1} - symmetric C—H. Peaks at 1131 cm^{-1} and 1092 cm^{-1} correspond to out-of-plane bending, 739 cm^{-1} - out-of-plane C═O bending [39]. The strong peak at 871 cm^{-1} assigned to C-COO stretching, 394 cm^{-1} to C-CO bending, and 299 cm^{-1} to C-O-C and C-CH bending [40,41]. GO incorporation influence the same way as for PCL, overlapping the scaffold bands, showing D and G peaks at 1328 cm^{-1} and 1588 cm^{-1} respectively with an I_D/I_G ratio of 1.17.

3.3. PLGA & PLC

PLGA and PLC are polymer materials that are also widely used in drug delivery systems and implant applications. As these polymers represent the same as PLLA family of homo and *co*-polymers originated from lactic and glycolic acid monomers - the obtained IR and RS vibration modes are very similar to PLLA, varying only in terms of intensity values. The most important characteristic bands, which allow identifying these polymers are represented by carbonyl stretching and C—H stretching vibrations for both cases [42]. The GO hydrophilicity "activation" of all the scaffolds surfaces is experimentally proved to be caused by the O—H group incorporation. Our systematic study demonstrates that the difference between contact angle values for plasma-treated and GO-functionalized plasma-treated scaffolds by the end of the monitoring month turned to be 58° ± 2° and 67° ± 4° for PLGA and PLC scaffolds, respectively (Figs. 1(c) and (d)). Notice that for all three GO-coated polymer types there is a contact angle difference for polymers with and without plasma treatment, which shows that the

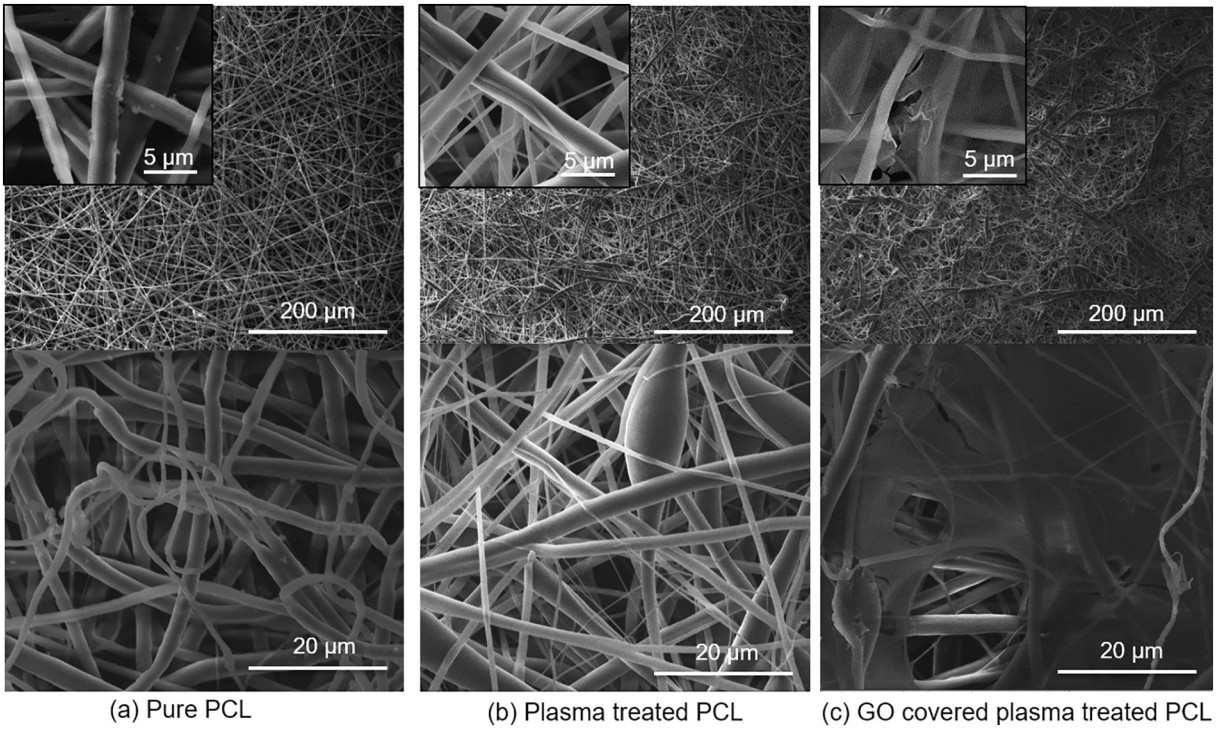

Fig. 2. SEM images of the PCL scaffolds performed with different magnification. (a) represents untreated scaffolds, (b) - scaffolds after plasma treatment only, (c) demonstrates the effect of both - plasma treatment and GO coating.

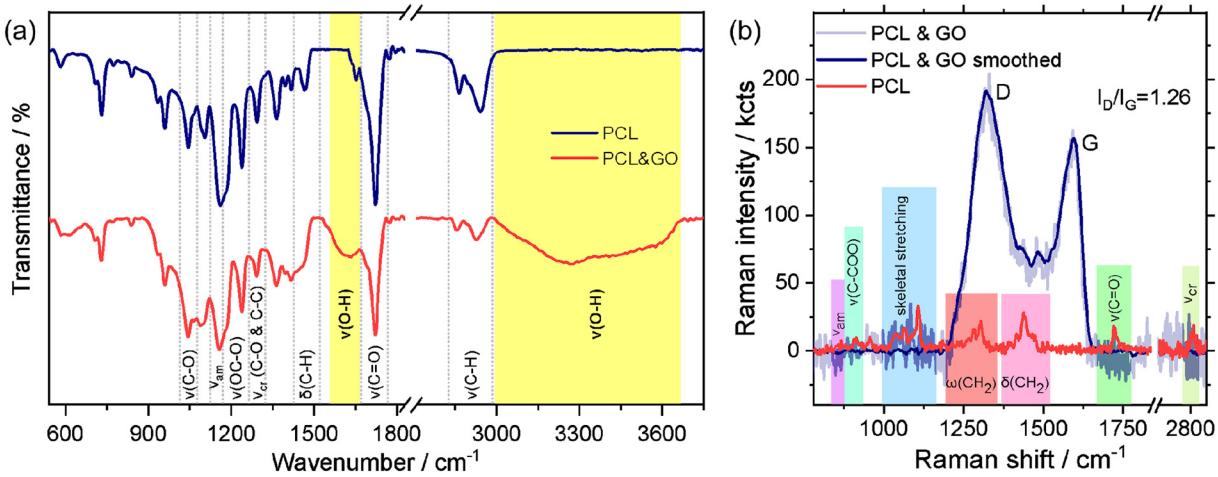

Fig. 3. Spectra of plasma-treated PCL scaffolds and GO-covered plasma-treated scaffolds, (a) FTIR and (b) Raman spectra.

GO/scaffold interaction plays a role in scaffold hydrophilicity. This is especially noticeable in the case of PLLA with lower values for plasma-treated samples than for untreated ones. This observation further confirms the efficiency of combining plasma treatment with GO functionalization.

The time-dependent evolution of contact angle results in Fig. 1 show an increase within the first week. This increase in contact angle can be attributed to a partial reduction of GO in room conditions. This explanation is in agreement with a preliminary report showing the partial reduction of multilayer GO already at 75 °C due to the presence of water [43]. At room temperature condition this process could take several days. We could quench the low contact angle observed right after GO deposition by treating the GO film with ethanol as shown by Acik et al. [43]. Nevertheless, the most significant observation is that all GO-functionalized scaffolds here investigated remained hydrophilic during the whole duration of this study. The slight changes of initial contact angle among PLLA, PLGA, and PLC shown in Fig. 1 could be related to small morphology and size variations among different polymer films [44]. The 1.33 I_D/I_G Raman intensity ratio of PLGA changes slightly from the other polymers studied above. However, for PLC the I_D/I_G ratio shifts to 0.96, at the same time showing a sharp G peak indicating the high graphitization of the sample. I_D/I_G Raman intensity ratio decrease indicates higher quality of the crystalline sp^2 structure after reduction [45]. In this regard, change for the GO-coated PLC scaffold suggests a possible reduction during the Raman spectroscopy analysis. Even if the laser power was the same for all samples, the heat dissipation could vary from sample to sample explaining the differences in GO reduction reflected by the different D/G intensity ratios [46].

Another important finding from the Raman spectroscopy results regards the GO thickness. We observe that for all samples the Raman signal from the polymer is not visible in the GO-coated suggesting a screening by the GO film. Given the low energy of the NIR laser used in

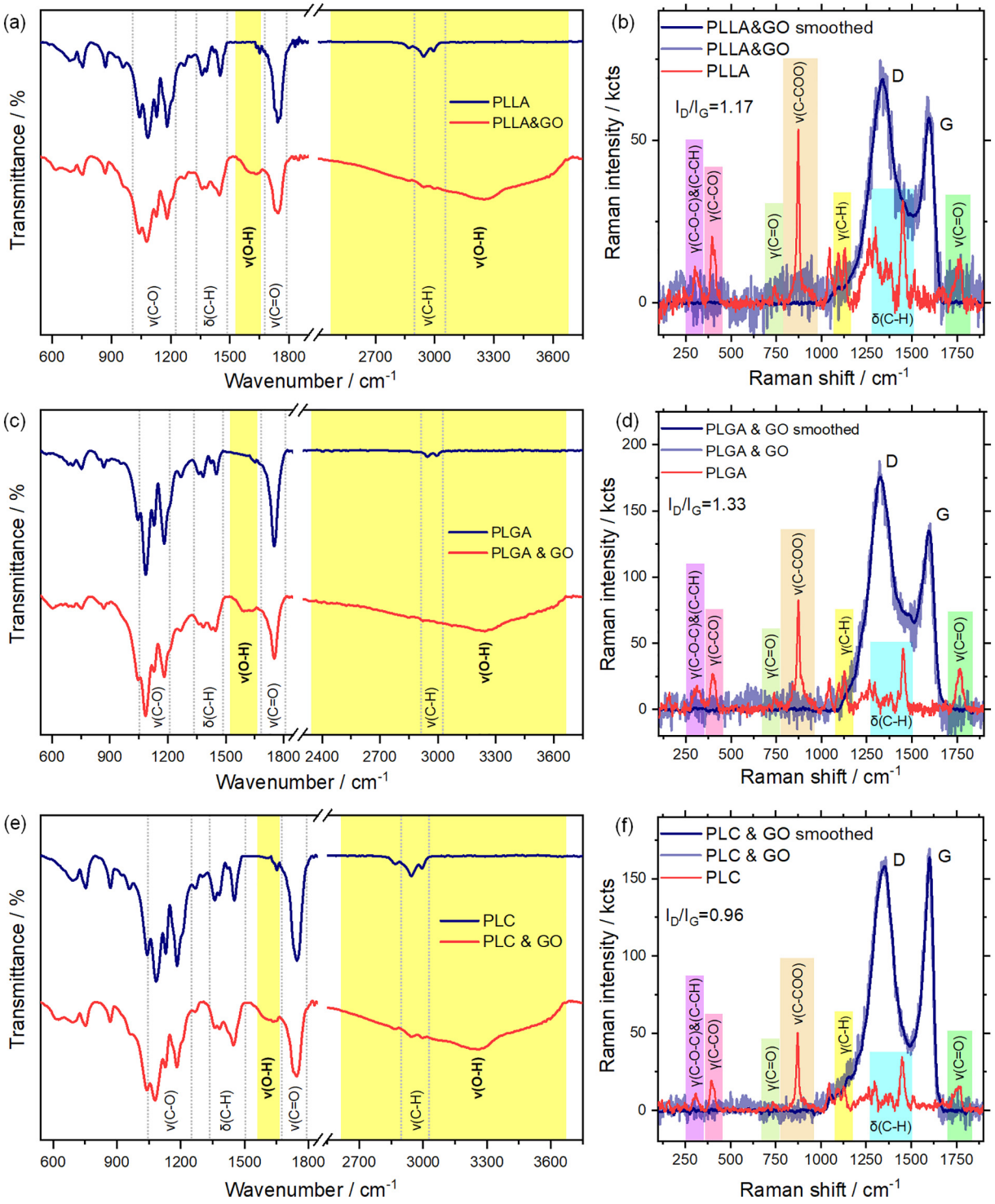

Fig. 4. Spectra of plasma-treated PLLA, PLGA, and PLC scaffolds and GO-covered plasma-treated scaffolds: (a) - PLLA Raman spectra (b) - PLLA FTIR spectra; (c) - PLGA Raman spectra (d) - PLGA FTIR spectra; (e) - PLC Raman spectra (f) - PLC FTIR spectra.

Raman, and the long penetration depth in GO at that energy [47], we can conclude that the GO functionalization resulted in the formation of a thick film.

4. Conclusions

Through this study a promising approach to overcome the hydrophobicity limitations of synthetic electrospun scaffolds by surface functionalization with GO was demonstrated. During the systematic study of four polymer types in the 30 days period, the long-term hydrophilic nature of GO-functionalized scaffolds was observed. This was contrary to the conventionally plasma-treated surfaces that already started to turn back hydrophobic within the first days. The GO-functionalized scaffolds display contact angle values after one month that did not exceed 41° among all samples (four polymer scaffolds types) indicating universality of the effect. The enhanced long-term wettability can be attributed to the hydroxyl groups from GO, resulting in a significant increase of polar groups. Characterization methods such as

FTIR and Raman helped to evaluate the changes taking place while functionalization and confirm the contribution of hydroxyl groups to the hydrophilic behavior. These results are promising for *in vitro* investigations to elucidate the long-term effects of GO-functionalized scaffolds in cell adhesion and proliferation which is now the subject of ongoing work.

CRediT authorship contribution statement

A. Lipovka: Investigation, Writing - original draft. **R. Rodriguez:** Conceptualization, Data curation. **E. Bolbasov:** Investigation, Writing - review & editing, Funding acquisition. **P. Maryin:** Investigation, Writing - review & editing. **S. Tverdokhlebov:** Funding acquisition, Conceptualization, Validation. **E. Sheremet:** Investigation, Writing - review & editing, Funding acquisition.

Declaration of competing interest

The authors declare that they have no known competing financial interests or personal relationships that could have appeared to influence the work reported in this paper.

Acknowledgments

The research was supported by Tomsk Polytechnic University within the framework of Tomsk Polytechnic University Competitiveness Enhancement Programs (VIU-RSCABS-142/2019) and Russian State Project “Science” (WSWW-2020-0011). The study of the spectral characteristics of materials in the infrared region was supported by the Russian Academy of Sciences (Fundamental Research Project no. AAAA-A19-119110690036-9). We acknowledge Ammar Al-Hamry and Varnika Prakash for providing the GO dispersion. All thanks Lyubov Krasnoshekova for the help with RS experiments, Nina Radishevskaya and the TPU center of collective use for operating FTIR, Valeriya Kudryavtseva and Vladimir Pichugin for providing and help with the drop shape analyzer, and Gennadiy Murastov for the help with the analysis and support.

Appendix A. Supplementary data

Supplementary data to this article can be found online at https://doi.org/10.1016/j.surfcoat.2020.125560.

References

[1] H. Tian, Z. Tang, X. Zhuang, X. Chen, X. Jing, Biodegradable synthetic polymers: preparation, functionalization and biomedical application, Prog. Polym. Sci. 37 (2012) 237–280, https://doi.org/10.1016/j.progpolymsci.2011.06.004.
[2] Q.P. Pham, U. Sharma, A.G. Mikos, Electrospinning of polymeric Nanofibers for tissue engineering applications: a review, Tissue Eng. 12 (2006) 1197–1211, https://doi.org/10.1089/ten.2006.12.1197.
[3] T. Jiang, E.J. Carbone, K.W.-H. Lo, C.T. Laurencin, Electrospinning of polymer nanofibers for tissue regeneration, Prog. Polym. Sci. 46 (2015) 1–24, https://doi.org/10.1016/j.progpolymsci.2014.12.001.
[4] M. Okamoto, B. John, Synthetic biopolymer nanocomposites for tissue engineering scaffolds, Prog. Polym. Sci. 38 (2013) 1487–1503, https://doi.org/10.1016/j.progpolymsci.2013.06.001.
[5] J. Ding, J. Zhang, J. Li, D. Li, C. Xiao, H. Xiao, H. Yang, X. Zhuang, X. Chen, Electrospun polymer biomaterials, Prog. Polym. Sci. 90 (2019) 1–34, https://doi.org/10.1016/j.progpolymsci.2019.01.002.
[6] H. Amani, H. Arzaghi, M. Bayandori, A.S. Dezfuli, H. Pazoki-Toroudi, A. Shafiee, L. Moradi, Controlling cell behavior through the Design of Biomaterial Surfaces: a focus on surface modification techniques, Adv. Mater. Interfaces 6 (2019) 1900572, , https://doi.org/10.1002/admi.201900572.
[7] D.G. Petlin, S.I. Tverdokhlebov, Y.G. Anissimov, Plasma treatment as an efficient tool for controlled drug release from polymeric materials: a review, J. Control. Release 266 (2017) 57–74, https://doi.org/10.1016/j.jconrel.2017.09.023.
[8] L. Chen, C. Yan, Z. Zheng, Functional polymer surfaces for controlling cell behaviors, Mater. Today (2017), https://doi.org/10.1016/j.mattod.2017.07.002.
[9] T.S. Demina, A.A. Frolova, A.V. Istomin, S.L. Kotova, M.S. Piskarev, K.N. Bardakova, M.Y. Yablokov, V.A. Altynov, L.I. Kravets, A.B. Gilman, T.A. Akopova, P.S. Timashev, Coating of polylactide films by chitosan: comparison of methods, J. Appl. Polym. Sci. 137 (2020) 48287, https://doi.org/10.1002/app.48287.
[10] G. Chen, P. Zhou, N. Mei, X. Chen, Z. Shao, L. Pan, C. Wu, Silk fibroin modified porous poly(ε-caprolactone) scaffold for human fibroblast culture in vitro, J. Mater. Sci. Mater. Med. 15 (2004) 671–677, https://doi.org/10.1023/B:JMSM.0000030208.89523.2a.
[11] S.I. Goreninskii, R.O. Guliaev, K.S. Stankevich, N.V. Danilenko, E.N. Bolbasov, A.S. Golovkin, A.I. Mishanin, V.D. Filimonov, S.I. Tverdokhlebov, “Solvent/non-solvent” treatment as a method for non-covalent immobilization of gelatin on the surface of poly(l-lactic acid) electrospun scaffolds, Colloids Surfaces B Biointerfaces 177 (2019) 137–140, https://doi.org/10.1016/j.colsurfb.2019.01.060.
[12] A. Ganjalinia, S. Akbari, A. Solouk, PLLA scaffolds surface-engineered via poly (propylene imine) dendrimers for improvement on its biocompatibility/controlled pH biodegradability, Appl. Surf. Sci. 394 (2017) 446–456, https://doi.org/10.1016/j.apsusc.2016.10.110.
[13] S. Khaliliazar, S. Akbari, M.H. Kish, Modification of poly(l-lactic acid) electrospun fibers and films with poly(propylene imine) dendrimer, Appl. Surf. Sci. 363 (2016) 593–603, https://doi.org/10.1016/j.apsusc.2015.12.070.
[14] R. Morent, N. De Geyter, T. Desmet, P. Dubruel, C. Leys, Plasma surface modification of biodegradable polymers: a review, Plasma Process. Polym. 8 (2011) 171–190, https://doi.org/10.1002/ppap.201000153.
[15] A.B. Gilman, T.S. Demina, P.S. Timashev, Plasmachemical surface modification to regulate biocompatibility of polymeric materials. Methods and setups, Perspekt. Mater. (2019) 5–19, https://doi.org/10.30791/1028-978X-2019-1-5-19.
[16] E.N. Bolbasov, L.V. Antonova, K.S. Stankevich, A. Ashrafov, V.G. Matveeva, E.A. Velikanova, Y.I. Khodyrevskaya, Y.A. Kudryavtseva, Y.G. Anissimov, S.I. Tverdokhlebov, L.S. Barbarash, The use of magnetron sputtering for the deposition of thin titanium coatings on the surface of bioresorbable electrospun fibrous scaffolds for vascular tissue engineering: a pilot study, Appl. Surf. Sci. 398 (2017) 63–72, https://doi.org/10.1016/j.apsusc.2016.12.033.
[17] D.V. Sidelev, M. Bestetti, G.A. Bleykher, V.P. Krivobokov, V.A. Grudinin, S. Franz, A. Vicenzo, Y.L. Shanenkova, Deposition of Cr films by hot target magnetron sputtering on biased substrates, Surf. Coatings Technol. 350 (2018) 560–568, https://doi.org/10.1016/j.surfcoat.2018.07.047.
[18] E.N. Bolbasov, P.V. Maryin, K.S. Stankevich, S.I. Goreninskii, V.L. Kudryavtseva, A.I. Mishanin, A.S. Golovkin, A.B. Malashicheva, Y.M. Zhukov, Y.G. Anissimov, S.I. Tverdokhlebov, Nitrogen-doped titanium dioxide thin films formation on the surface of PLLA electrospun microfibers scaffold by reactive magnetron sputtering method, Plasma Chem. Plasma Process. (2019), https://doi.org/10.1007/s11090-019-09956-x.
[19] E.N. Bolbasov, P.V. Maryin, K.S. Stankevich, A.I. Kozelskaya, E.V. Shesterikov, Y.I. Khodyrevskaya, M.V. Nasonova, D.K. Shishkova, Y.A. Kudryavtseva, Y.G. Anissimov, S.I. Tverdokhlebov, Surface modification of electrospun poly-(l-lactic) acid scaffolds by reactive magnetron sputtering, Colloids Surfaces B Biointerfaces 162 (2018) 43–51, https://doi.org/10.1016/j.colsurfb.2017.11.028.
[20] M.H.A. van Dongen, R.O.F. Verkuijlen, R. Aben, J.P.C. Bernards, Wettability and aging of polymer substrates after atmospheric Dielectrical barrier discharge plasma on demand treatment, J. Imaging Sci. Technol. 57 (2013) 1–5, https://doi.org/10.2352/J.ImagingSci.Technol.2013.57.3.030503.
[21] J.K.Y. Lee, N. Chen, S. Peng, L. Li, L. Tian, N. Thakor, S. Ramakrishna, Polymer-based composites by electrospinning: preparation & functionalization with nanocarbons, Prog. Polym. Sci. 86 (2018) 40–84, https://doi.org/10.1016/j.progpolymsci.2018.07.002.
[22] S. Goenka, V. Sant, S. Sant, Graphene-based nanomaterials for drug delivery and tissue engineering, J. Control. Release 173 (2014) 75–88, https://doi.org/10.1016/j.jconrel.2013.10.017.
[23] O.C. Compton, S.T. Nguyen, Graphene oxide, highly reduced Graphene oxide, and Graphene: versatile building blocks for carbon-based materials, Small 6 (2010) 711–723, https://doi.org/10.1002/smll.200901934.
[24] S. Pei, H.-M. Cheng, The reduction of graphene oxide, Carbon N. Y 50 (2012) 3210–3228, https://doi.org/10.1016/j.carbon.2011.11.010.
[25] L. Dedelaite, R.D. Rodriguez, E. Andriukonis, M. Hietschold, D.R.T. Zahn, A. Ramanavicius, Surfaces functionalized by graphene oxide nanosheets for single cell investigations, Sensors Actuators B Chem. 255 (2018) 1735–1743, https://doi.org/10.1016/j.snb.2017.08.187.
[26] W.C. Lee, C.H.Y.X. Lim, H. Shi, L.A.L. Tang, Y. Wang, C.T. Lim, K.P. Loh, Origin of enhanced stem cell growth and differentiation on Graphene and Graphene oxide, ACS Nano 5 (2011) 7334–7341, https://doi.org/10.1021/nn202190c.
[27] K. Zhang, H. Zheng, S. Liang, C. Gao, Aligned PLLA nanofibrous scaffolds coated with graphene oxide for promoting neural cell growth, Acta Biomater. 37 (2016) 131–142, https://doi.org/10.1016/j.actbio.2016.04.008.
[28] Z. Wang, H. Shen, S. Song, L. Zhang, W. Chen, J. Dai, Z. Zhang, Graphene oxide incorporated PLGA Nanofibrous scaffold for solid phase gene delivery into Mesenchymal stem cells, J. Nanosci. Nanotechnol. 18 (2018) 2286–2293, https://doi.org/10.1166/jnn.2018.14362.
[29] E. Malikmammadov, T.E. Tanir, A. Kiziltay, V. Hasirci, N. Hasirci, PCL and PCL-based materials in biomedical applications, J. Biomater. Sci. Polym. Ed. (2017) 1–31, https://doi.org/10.1080/09205063.2017.1394711.
[30] T. Elzein, M. Nasser-Eddine, C. Delaite, S. Bistac, P. Dumas, FTIR study of polycaprolactone chain organization at interfaces, J. Colloid Interface Sci. 273 (2004) 381–387, https://doi.org/10.1016/j.jcis.2004.02.001.
[31] S.H. Murphy, G.A. Leeke, M.J. Jenkins, A comparison of the use of FTIR spectroscopy with DSC in the characterisation of melting and crystallisation in polycaprolactone, J. Therm. Anal. Calorim. 107 (2012) 669–674, https://doi.org/10.1007/s10973-011-1771-7.
[32] C.H. Manoratne, S.R.D. Rosa, I.R.M. Kottegoda, XRD-HTA, UV visible, FTIR and

SEM interpretation of reduced Graphene oxide synthesized from high purity vein graphite, Mater. Sci. Res. India 14 (2017) 19–30, https://doi.org/10.13005/msri/140104.
[33] K. Wang, J. Ruan, H. Song, J. Zhang, Y. Wo, S. Guo, D. Cui, Biocompatibility of Graphene oxide, Nanoscale Res. Lett. (2010), https://doi.org/10.1007/s11671-010-9751-6.
[34] B.D. Ossonon, D. Bélanger, Synthesis and characterization of sulfophenyl-functionalized reduced graphene oxide sheets, RSC Adv. 7 (2017) 27224–27234, https://doi.org/10.1039/C6RA28311J.
[35] A.P. Kotula, C.R. Snyder, K.B. Migler, Determining conformational order and crystallinity in polycaprolactone via Raman spectroscopy, Polymer (Guildf) 117 (2017) 1–10, https://doi.org/10.1016/j.polymer.2017.04.006.
[36] M.M. Kadam, O.R. Lokare, K.V.M.K. Kireeti, V.G. Gaikar, N. Jha, Impact of the degree of functionalization of graphene oxide on the electrochemical charge storage property and metal ion adsorption, RSC Adv. 4 (2014) 62737–62745, https://doi.org/10.1039/C4RA08862J.
[37] A.J.R. Lasprilla, G.A.R. Martinez, B.H. Lunelli, A.L. Jardini, R.M. Filho, Poly-lactic acid synthesis for application in biomedical devices — a review, Biotechnol. Adv. 30 (2012) 321–328, https://doi.org/10.1016/j.biotechadv.2011.06.019.
[38] V. Krikorian, D. Pochan, Crystallization behavior of poly(lactic acid) nanocomposites: nucleation and growth probed by infrared spectroscopy, Macromolecules 38 (2005) 6520–6527, https://doi.org/10.1021/ma050739z.
[39] T. Suzuki, A. Ei, Y. Takada, H. Uehara, T. Yamanobe, K. Takahashi, Modification of physical properties of poly(L-lactic acid) by addition of methyl-β-cyclodextrin, Beilstein J. Org. Chem. 10 (2014) 2997–3006, https://doi.org/10.3762/bjoc.10.318.
[40] M. Radjabian, M.H. Kish, N. Mohammadi, Characterization of poly(lactic acid) multifilament yarns. I. the structure and thermal behavior, J. Appl. Polym. Sci. 117 (2010) 1516–1525, https://doi.org/10.1002/app.32046.
[41] M.A. Cuiffo, J. Snyder, A.M. Elliott, N. Romero, S. Kannan, G.P. Halada, Impact of the fused deposition (FDM) printing process on Polylactic acid (PLA) chemistry and structure, Appl. Sci. 7 (2017) 579, https://doi.org/10.3390/app7060579.
[42] H. Keles, A. Naylor, F. Clegg, C. Sammon, Studying the release of hGH from gamma-irradiated PLGA microparticles using ATR-FTIR imaging, Vib. Spectrosc. 71 (2014) 76–84, https://doi.org/10.1016/j.vibspec.2014.01.012.
[43] M. Acik, C. Mattevi, C. Gong, G. Lee, K. Cho, M. Chhowalla, Y.J. Chabal, The role of intercalated water in multilayered Graphene oxide, ACS Nano 4 (2010) 5861–5868, https://doi.org/10.1021/nn101844t.
[44] R. Ghobeira, M. Asadian, C. Vercruysse, H. Declercq, N. De Geyter, R. Morent, Wide-ranging diameter scale of random and highly aligned PCL fibers electrospun using controlled working parameters, Polymer (Guildf) 157 (2018) 19–31, https://doi.org/10.1016/j.polymer.2018.10.022.
[45] H. Yang, H. Hu, Y. Wang, T. Yu, Rapid and non-destructive identification of graphene oxide thickness using white light contrast spectroscopy, Carbon N. Y. 52 (2013) 528–534, https://doi.org/10.1016/j.carbon.2012.10.005.
[46] B. Ma, R.D. Rodriguez, E. Bogatova, A. Ruban, S. Turanov, D. Valiev, E. Sheremet, Non-invasive monitoring of red beet development, Spectrochim. Acta Part A Mol. Biomol. Spectrosc. 212 (2019) 155–159, https://doi.org/10.1016/j.saa.2019.01.006.
[47] V.H. Pham, T.V. Cuong, S.H. Hur, E. Oh, E.J. Kim, E.W. Shin, J.S. Chung, Chemical functionalization of graphene sheets by solvothermal reduction of a graphene oxide suspension in N-methyl-2-pyrrolidone, J. Mater. Chem. 21 (2011) 3371–3377, https://doi.org/10.1039/C0JM02790A.